Materials Science and Engineering B 174 (2010) 31–37

Contents lists available at ScienceDirect

Materials Science and Engineering B

journal homepage: www.elsevier.com/locate/mseb

Electrical and optical properties of ultrasonically sprayed Al-doped zinc oxide thin films

B.J. Babu*, A. Maldonado, S. Velumani, R. Asomoza

Department of Electrical Engineering-SEES, CINVESTAV-IPN, Zacatenco, D.F., C.P. 07360, Mexico

ARTICLE INFO

Article history:
Received 3 September 2009
Received in revised form 4 February 2010
Accepted 7 March 2010

Keywords:
AZO
USP
Electrical and optical properties
XRD
FESEM

ABSTRACT

Aluminium-doped ZnO (AZO) films were deposited by ultrasonic spray pyrolysis (USP) technique to investigate its potential application as antireflection coating and top contact layer for copper indium gallium diselenide (CIGS) based photovoltaic cells. The solution used to prepare AZO thin films contained 0.2 M of zinc acetate and 0.2 M of aluminium pentanedionate solutions in the order of 2, 3 and 4 at.% of Al/Zn. AZO films were deposited onto glass substrates at different substrate temperatures starting from 450 °C to 500 °C. XRD and FESEM analysis revealed the structural properties of the films and almost all the films possessed crystalline structure with a preferred (0 0 2) orientation except for the 4 at.% of Al. Grain size of AZO films varied from 29.7 to 37 nm for different substrate temperatures and atomic percentage of aluminium. The average optical transmittance of all films with the variation of doping concentration and substrate temperature was 75–90% in the visible range of wavelength 600–700 nm. Optical direct band gap value of 2, 3 and 4 at.% Al-doped films sprayed at different temperatures varied from 3.32 to 3.46 eV. Hall studies were carried out to analyze resistivity, mobility and carrier concentration of the films. AZO films deposited at different substrate temperatures and at various Al/Zn ratios showed resistivity ranging from 0.12 to 1.0×10^{-2} Ω cm. Mobility value was ~5 $cm^2/V\,s$ and carrier concentration value was ~7.7×10^{19} cm^{-3}. Minimum electrical resistivity was obtained for the 3 at.% Al-doped film sprayed at 475 °C and its value was 1.0×10^{-2} Ω cm with film thickness of 602 nm. The electrical conductivity of ZnO films was improved by aluminium doping.

1. Introduction

ZnO is a II–VI group semiconductor material with wide direct band gap and wurtzite structure. The high stability, melting point and excitation energy makes it a promising ultraviolet (UV) and blue optoelectronic material. In addition, ZnO thin films offer a variety of applications in solar cells, optoelectronic, and gas sensitive devices [1]. A transparent conducting electrode is a necessary component in all flat panel displays (FPDs). Commercially most important material for a transparent conducting film nowadays is Sn-doped In_2O_3 (ITO), owing to its unique characteristics of high visible transmittance (90%), low DC resistivity, high infrared reflectance and absorbance in the microwave region. The high quality of ITO films deposited by sputtering of oxide targets has already been successfully achieved on a commercialized production scale [2]. On the other hand, ZnO films have attracted interest as a transparent conductive coating material, because of the materials characteristics such as (1) cheap and abundant element, (2) production of large-scale coatings, (3) allow tailing of ultraviolet absorption, (4) high stability in hydrogen plasma, (5) low growth temperature, (6) nontoxic and (7) easy to fabricate. Electrical resistivity of ZnO thin film is readily modified by the addition of impurity or post-deposition annealing [2,3]. Aluminum-doped zinc oxide (AZO) thin films have been prepared by thermal evaporation [4], chemical vapour deposition (CVD) [5], sol–gel [6,7], pulsed laser deposition (PLD) [8] magnetron sputtering [2,9], and spray pyrolysis [3,10–17], etc.

Among these methods, spray pyrolysis is cheap and useful for large area applications. This method is simpler, fast, material efficient, easy to use, carried out in non-vacuum system and permits to obtain films with the required properties for optoelectronic applications. In the ultrasonic spray pyrolysis (USP) system, an alcoholic solution containing the precursor-salts is nebulized by an ultrasonic actuator and then transported to a heated substrate. The advantage of USP over conventional pneumatic spraying is low consumption of material, and better control of the spray flux with a soft carrier-gas flow, which allows the deposition of very thin layers with homogeneous thickness. Already reports are available on the In_2S_3 thin buffer layers deposited by USP over CIGS layers in solar cells, where the desired film thickness is in nano-scale [15,16]. Since not many systematic reports are available on the USP deposition of AZO thin films, this study reports the effect of [Al]/[Zn] ratio in

* Corresponding author. Tel.: +52 55 5747 4001; fax: +52 55 5747 4003.
E-mail address: jbabu@cinvestav.mx (B.J. Babu).

0921-5107/$ – see front matter © 2010 Elsevier B.V. All rights reserved.
doi:10.1016/j.mseb.2010.03.010

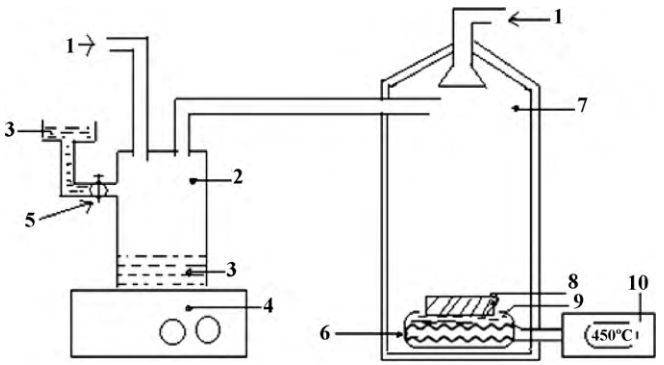

Fig. 1. Experimental setup of ultrasonic spray pyrolysis method (1, carrier gas pipe; 2, container; 3, solution; 4, ultrasonic nebulizer; 5, valve; 6, heating system; 7, deposition room; 8, substrate; 9, tin bath; 10, temperature controller).

the starting solution and substrate temperature on the optical and electrical characteristics of these thin films which are explored for its application in photovoltaic devices as transparent conducting oxide contact.

2. Experimental details

Al-doped ZnO thin films were prepared by ultrasonic spray pyrolysis method. An ultrasonic spray pyrolytic apparatus (vertical configuration type) was used. A schematic of homemade experimental setup is shown in Fig. 1. 0.2 M starting solution was prepared from zinc acetate dehydrate ($Zn(CH_3COO)_2{\cdot}2H_2O$) (Merck) dissolved in methanol (Baker) and acetic acid (Merck). Aluminum pentanedionate ($C_{15}H_{21}AlO_6$) (Alfa) previously diluted in deionized water and acetic acid (Merck) at 0.2 M was added to the Zn solution in order to dope the initial solution such that [Al/Zn] ratio to be 2, 3 and 4 at.%. The solution was sprayed onto previously cleaned soda lime glass substrates. Droplets of solution produced by the ultrasonic generator were carried to the substrate by nitrogen gas. The films were deposited in air at temperatures ranging from 450 °C to 500 °C for 10 min. Structural analysis of films was performed by PANalytical X-ray diffractometer with CuKα (λ = 1.5406 Å) radiation. SEM micrographs of the films have been taken using JEOL JSM-7401F FESEM. Transmittance spectra were obtained using SHIMADZU UV–vis double beam spectrophotometer in the wavelength range 300–1100 nm. The film thickness was measured by a KLA Tencor P15 profilometer, etching an edge of the sample to make a reference step. Hall measurements were carried out by the Van der Pauw method using a Walker scientific HV-4H equipment.

3. Results and discussion

When aerosol droplets arrive close to the heated glass substrates, a pyrolytic process takes place and a highly adherent film of ZnO forms on the substrates. Possible reaction mechanism for the ZnO thin films deposited by spray pyrolysis has been reported by Paraguay et al. [18]. In the present work similar kind of reaction mechanism takes place except for the replacement of zinc atoms by aluminium atoms. Fig. 2 shows simulated pattern of the ZnO structure incorporated with aluminium. AZO structure is simulated using Material Studio program considering space group as *P*63*mc*, lattice parameters $a = b = 3.2533$, $c = 5.2073$; $\alpha = \beta = 90°$, $\gamma = 120°$ (hexagonal) and zinc atoms stay at 1/3, 2/3, 0; oxygen atoms at 1/3, 2/3, 0.3820. From Fig. 2 it is evident that Zn atoms are replaced by aluminium atoms.

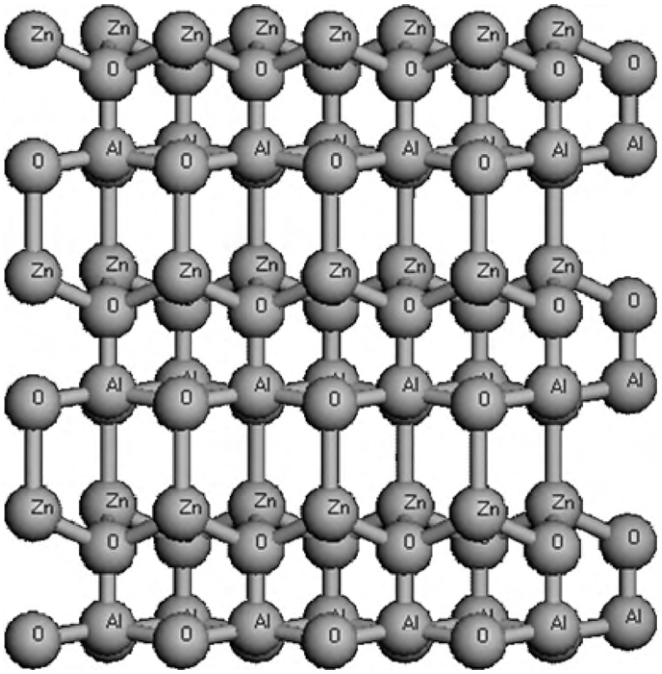

Fig. 2. Stimulated pattern of ZnO structure incorporated with aluminium.

3.1. Structural properties

3.1.1. X-ray diffraction (XRD)

Structural characterization is very important to know the crystal structure and orientation of the films and also to explain optical and electrical properties of these films. It is known that crystallite size is the deterministic factor affecting the enhancement of conductivity [12,19] and optical transmission [6] of the films. The structural developments of AZO films deposited for 2, 3 and 4 at.% Al/Zn ratio as a function of different deposition temperatures ranging from 450 °C to 500 °C are shown in Fig. 3a–c. As the substrate temperature increased, the peak intensity and crystal size increased, which may be due to the decrease in stress with increasing temperature. All films were polycrystalline with a structure that belongs to the ZnO hexagonal wurtzite type [JCPDS, 36-1451]. An increase in peak intensity associated with the (1 0 1) planes is found for Al-doped ZnO thin films and no diffraction peaks of Al_2O_3 or other impurities were observed [7,11]. In all cases a preferential (0 0 2) growth appears indicating that the crystallite structure of films is oriented with their *c*-axis perpendicular to the substrate, irrespective of Al/Zn content [14] except for the 4 at.% Al films, where it was observed to have orientation along (1 0 1). It was observed that with the increase in deposition temperature the intensity of (0 0 2) peak increased for 2 and 3 at.% but for 4 at.% the preferential orientation changed from (1 0 1) to (1 0 0) at higher temperatures. However the intensity of (0 0 2) peak decreased by increasing the doping concentration.

Grain size of AZO films varied from 29.7 to 37 nm for different substrate temperatures and atomic percentage of aluminium. The grain size increased with increase in substrate temperature for all doping concentrations whereas it increased up to a critical doping concentration of 3 at.% Al and then decreased for still higher doping concentrations. An increase in doping concentration deteriorates the crystallinity of films, which may be due to the formation of stress induced by ion size difference between zinc and aluminium ($r_{Zn^{2+}} = 0.074$ nm and $r_{Al^{3+}} = 0.054$ nm) and the segregation of aluminium in grain boundaries for high doping concentrations [3,6–8]. Similar behavior was observed by Liu et al. [10]

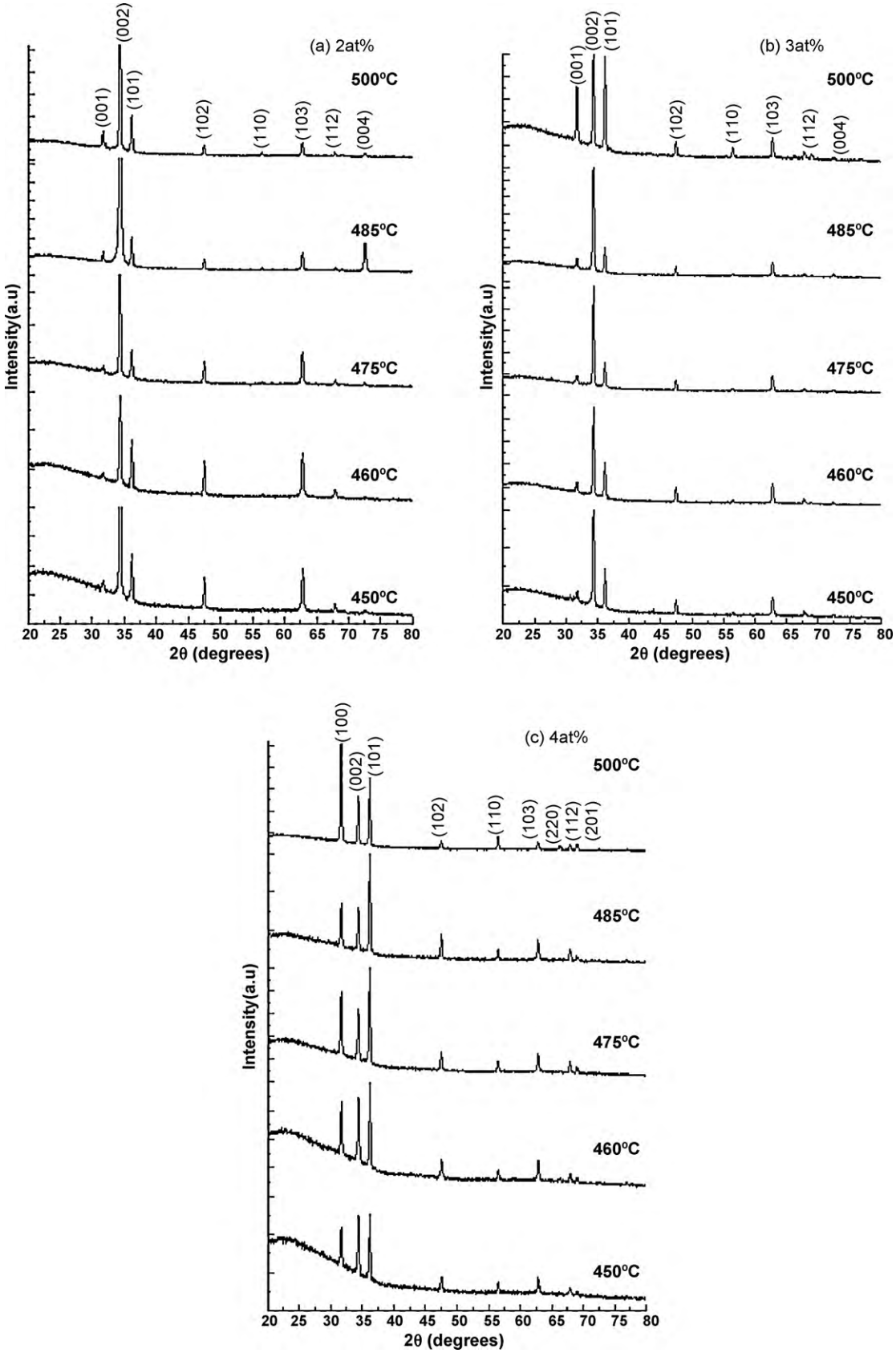

Fig. 3. XRD patterns of AZO thin films for (a) 2 at.%, (b) 3 at.%, and (c) 4 at.% deposited at various deposition temperatures.

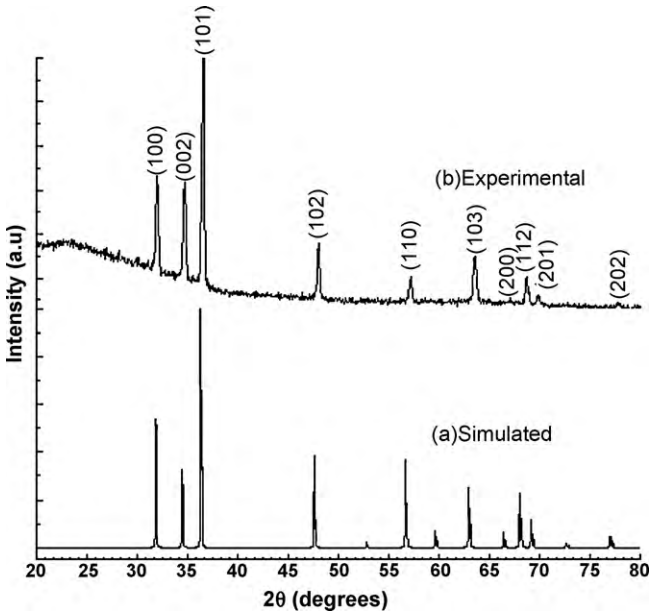

Fig. 4. Comparisons between XRD patterns of (a) simulated and (b) experimental AZO structure.

in the case of ZnO:Ag films grown by USP and Prathap et al. [20] in ZnS:Al films. The extra aluminum atoms might not occupy the appropriate sites inside the zinc oxide crystallites because of the limited solubility of aluminium in ZnO. This aluminium excess may occupy interstitial positions and then deform the crystal structure [21]. Grain size decreased with increase in doping concentration due to the effect of Al on the nucleation and coalescence of islands during the process of film growth [20] and also decrease in the preferred orientation with a reduced grain diameter was noticed with the increasing Al concentration. Similar pattern was noticed by Atay et al. [22] in CdS:Ni films deposited by USP and also Yakuphanoglu et al. [23] observed for fluorine doped ZnO thin films. However, non-optimal experimental conditions, defects and other chemical impurities (i.e., in this case doping) may hinder the (0 0 2)-oriented growth as seen in Fig. 3c for 4 at.% [24]. Fig. 4a and b gives a comparison between XRD patterns of simulated AZO structure (Fig. 2) and the film deposited at 485 °C with 4 at.% aluminium. Simulated XRD pattern is found to be in good agreement with the experimental pattern and the simulated pattern exactly matches with all the peaks found in experimental pattern.

3.2. Surface morphology

3.2.1. Field emission scanning electron microscopy (FESEM)

FESEM images of AZO thin films deposited at 475 °C with 2, 3 and 4 at.% of Al/Zn ratio are shown in Fig. 5a–c. These images show that the surface morphology of the films is strongly dependent on the concentration of aluminium. As it can be seen from micrographs, grain size varied as doping concentration increased due to the difference in ionic radius of zinc and aluminium [6]. At higher Al/Zn concentrations, the development of agglomerates from the small spiral grains (Fig. 5a) gives rise to elongated secondary grains as observed in Fig. 5b. After critical aluminium concentration, Al tends to segregate at the grain boundaries, hindering the development of longer grains as shown in Fig. 5c [14].

3.3. Optical properties

The effects of doping aluminium concentrations and substrate temperatures on the optical transmittance of AZO thin films are

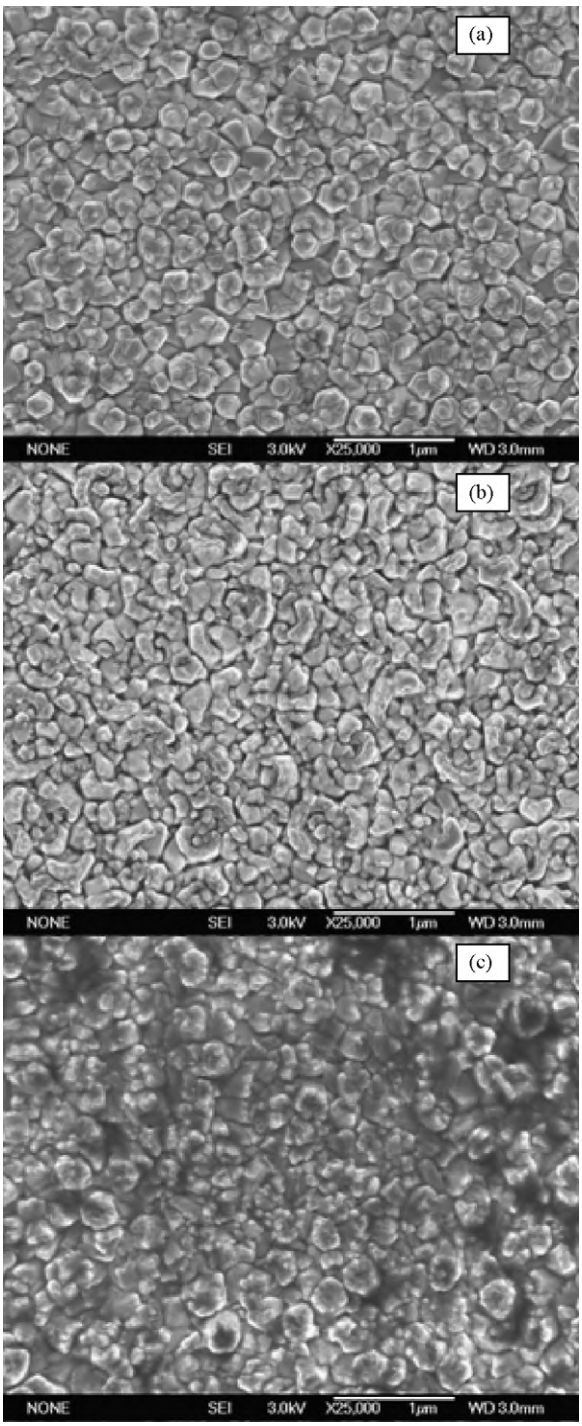

Fig. 5. FESEM images of AZO thin films deposited at 475 °C with (a) 2 at.%, (b) 3 at.% and (c) 4 at.% of Al/Zn.

presented in Fig. 6a–c. The transmittance of films varied with temperature, maximum transmittance is observed for films deposited at 450 °C. The optical transmittance of all films with various doping concentrations and substrate temperatures was found to vary from 75 to 90% in the visible range of wavelength 600–700 nm. Transmittance of the doped film with 2 at.% Al at 450 °C is near 90% and is higher than that of the doped film with 3 and 4 at.%. This may be due to the fact that the film with 2 at.% doping presents more voids than the films with 3 and 4 at.% doping, which may lead to a decrease in optical scattering and increase in transmittance [6]. The optical transmittance of films is known to be dependent upon

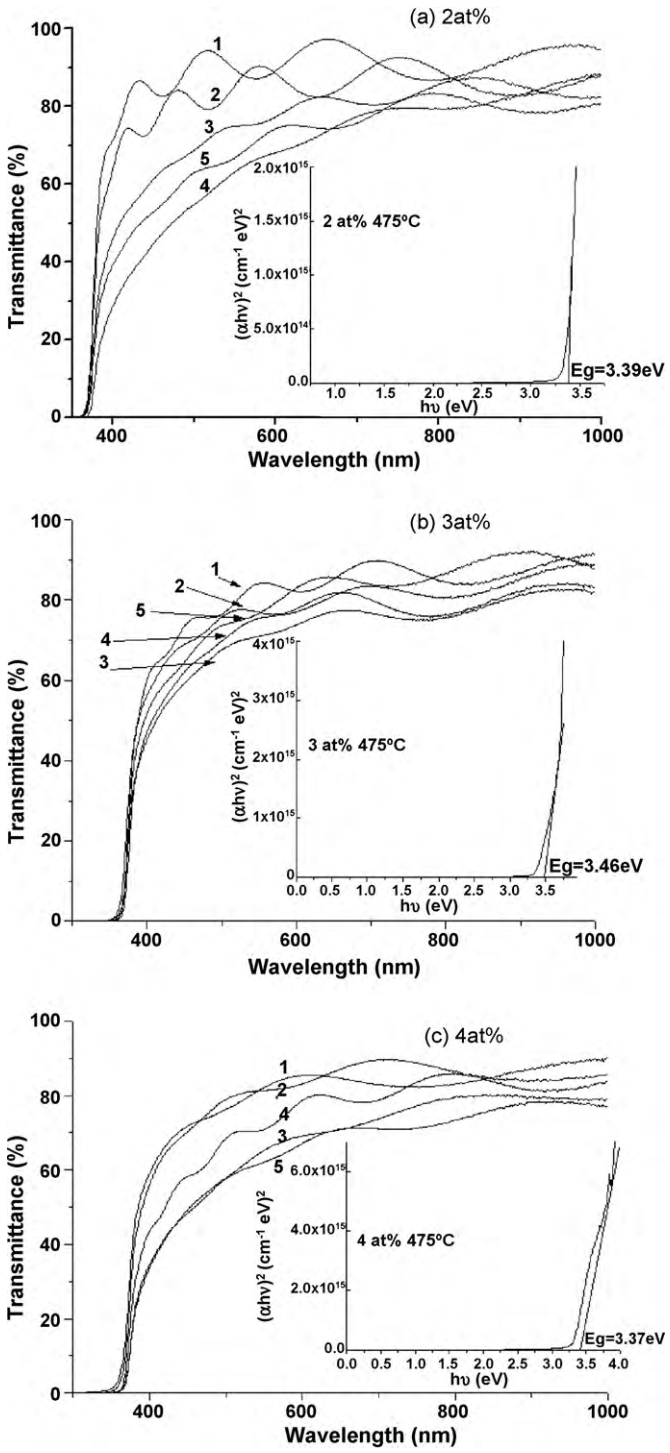

Fig. 6. The effects of doping aluminium concentrations: (a) 2 at.%, (b) 3 at.% and (c) 4 at.% and substrate temperatures (1) 450 °C, (2) 460 °C, (3) 475 °C, (4) 485 °C and (5) 500 °C on the optical transmittance of the AZO thin films. Inset figure shows $(\alpha h\upsilon)^2$–$h\upsilon$ graph for AZO film.

the surface morphology [3]. At higher aluminium concentrations the films tend to be powdery in nature and whitish in appearance [25] as in the case of 4 at.% FESEM image (Fig. 5c). The decrease of transmittance at higher doping levels may be attributed to the increased scattering of photons by crystal defects created by doping. The free carrier absorption of the photons may also contribute to the observed reduction in the optical transmission of heavily doped films [26].

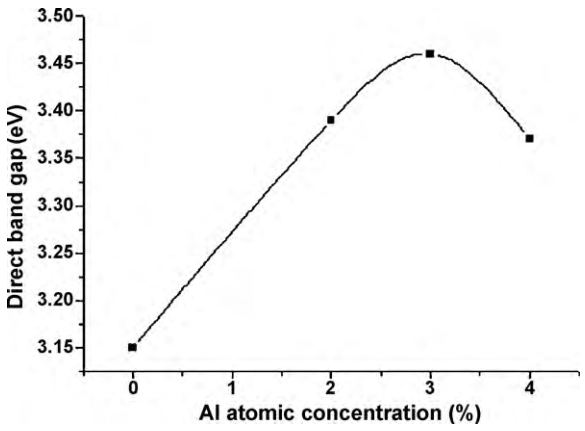

Fig. 7. Variation of optical direct band gap with change in aluminium concentration for the films deposited at 475 °C.

The other important optical parameter is the band gap of materials. Band gap values are obtained by extrapolating the linear portion in the plots of $(\alpha h\upsilon)^2$ versus $(h\upsilon)$ to cut the x-axis, i.e., at $(\alpha h\upsilon)^2 = 0$ as given in Fig. 6(inset). First of all, from the plot it was determined that the film has direct band gap, and this property is suitable for photovoltaic applications [27]. Secondly, the optical direct band gap value of 2, 3 and 4 at.% Al-doped films sprayed at different temperatures varied from 3.32 to 3.46 eV.

Increment in the direct band gap value of AZO films by doping of aluminium may be attributed to the Burstein–Moss effect [3] in which the optical direct band gap increased followed by heavy dopant concentration. Fig. 7 shows variation of optical direct band gap with the change in aluminium concentration for the films deposited at 475 °C. In our case it is observed that a decrease in band gap after 3 at.% Al doping, this is attributed to anomalous behavior of the optical band gap of nanocrystalline zinc oxide thin films [28]. According to Srikant and Clarke [28] Burstein–Moss effect is valid for materials having low effective mass of electrons and holes. Quantum confinement leads to the initial rise in the optical band gap. On increasing the carrier concentration to the critical value, the potential at the grain boundaries collapse, leading to an abrupt decrease in the optical band gap. Above this carrier concentration the films behave according to existing many-body theories. In the case of ZnO films grown by Srikant and Clarke [28] finite potential at the grain boundaries is 0.1 eV and the small grain sizes (50 nm), the electrons in the grains experience quantum confinement. In our case grain size is in the range of 29–37 nm, thus quantum confinement affect is expected. Quantum confinement has primarily two consequences. First, it splits the conduction band into discrete levels, and secondly, it reduces the density of states available in the conduction band [28].

3.4. Electrical properties

Besides the optical properties, electrical properties are also an important aspect of the performance of AZO thin films. The effects of doping aluminium concentration and substrate temperature on the electrical resistivity, mobility and carrier concentration of the doped ZnO thin films are presented in Fig. 8a–c. In all the cases, the resistivity of film decreases as the growth temperature increases from 450 °C to 475 °C respectively. After this, the resistivity increases from 475 °C to 500 °C. Growth temperature also affects the carrier concentration and mobility of the films. It is observed that the carrier concentration and the mobility of the films first increase with increase in growth temperature and then decrease with temperature. AZO films deposited at different substrate temperatures and at various Al/Zn ratios showed resistivity ranging

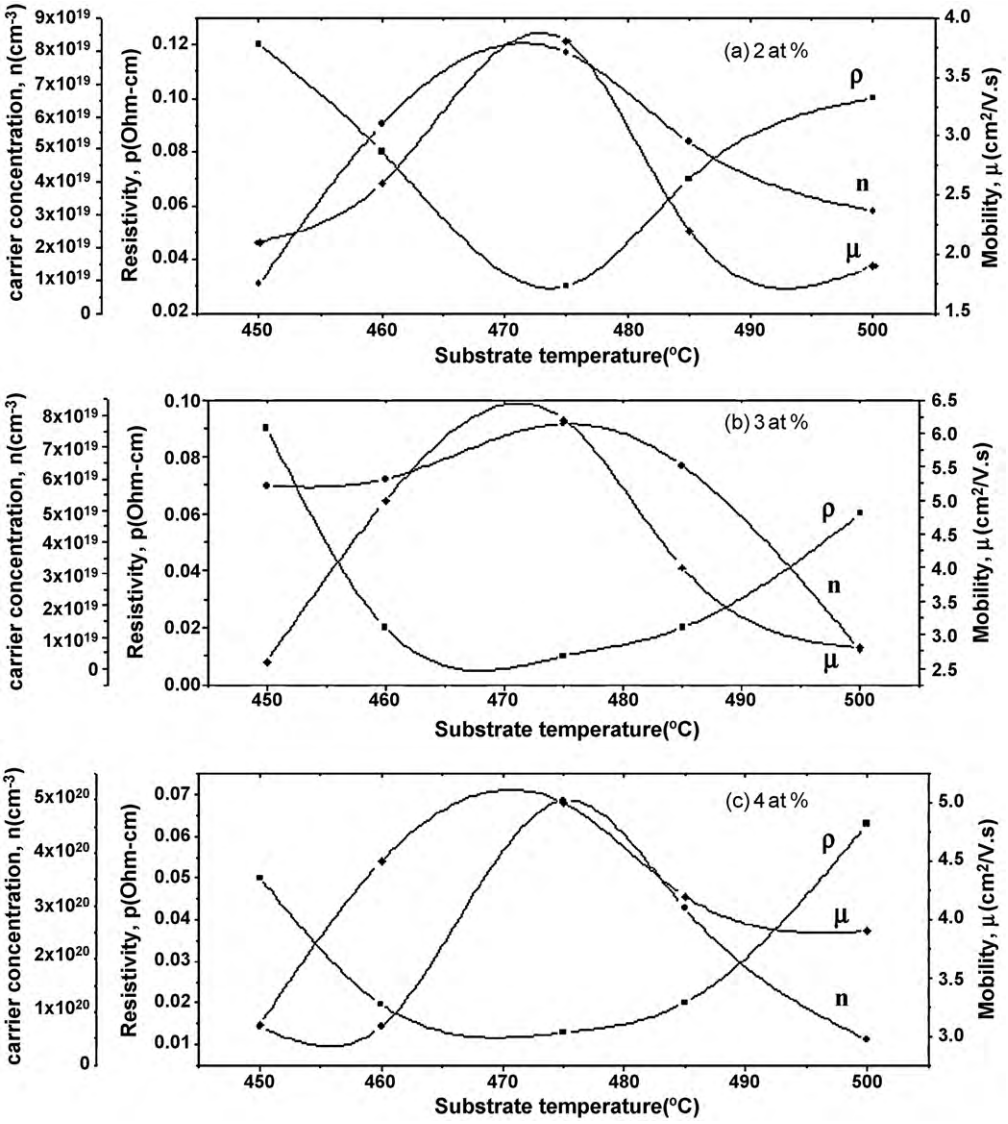

Fig. 8. The effects of aluminium concentrations: (a) 2 at.%, (b) 3 at.% and (c) 4 at.% and substrate temperature on the electrical resistivity (ρ), mobility (μ) and carrier concentration (n).

from 0.12 to $1.0 \times 10^{-2}\ \Omega$ cm. Mobility value was $\sim$5 $cm^2/V\,s$ and carrier concentration value was $\sim 7.7 \times 10^{19}\ cm^{-3}$. At higher temperatures, decrease in the content of oxygen vacancies or zinc interstitials, leads to a more stable material with high resistivity. In addition, the effects of out-diffusion of alkaline impurities coming from the substrate are promoted at high substrate temperature regime compensating the donor character of the impurities [29].

By comparison of resistivity of three different compositions of aluminium, minimum resistivity is found for 3 at.% film deposited at 475 °C. An increase in resistivity at higher doping concentrations is because, when a small amount of Al was introduced into the ZnO film, the Al was ionized into Al^{3+} and substituted for Zn^{2+}. Thus, one free electron was produced from one zinc atom replacement by an aluminum atom [29]. The carrier concentration increased with the Al concentration up to 3 at.%. At more than 3 at.%, however, the carrier concentration decreased because the increasing Al atoms formed some kind of neutral defects and these neutralized Al atoms did not contribute free electrons [3].

According to Yanfeng et al. [30], oxygen atoms were prone to form Na zeolite structure which could create more neutral impurity scattering center in the low and high-temperature range except for the middle one, so the influence of the scattering would be enhanced. As a result, Hall mobility and carrier concentration decreased.

Amount of electrically active Al in the film was reduced when the Al doping is high. Also this result is a consequence of aluminium solubility into the ZnO lattice, which is limited up to certain value (in this case 3 at.%), beyond this value it is supposed that the excess aluminium is segregated at the grain boundaries, as seen in Fig. 5c and thus increasing the barrier height and consequently reducing the electron mobility and carrier concentration [6,14].

4. Conclusions

Al-doped ZnO (AZO) films were successfully prepared by a homemade ultrasonic spray pyrolysis (USP) technique. The effects of substrate temperature and aluminium concentration on the electrical and optical characteristics of AZO thin films were studied. XRD analysis shows that the sprayed AZO thin films are of polycrystalline texture with a hexagonal structure. FESEM analyses revealed polycrystalline morphology of the films. Optical transmittance at 600–700 nm ranged from 75 to 90%, depending on the substrate temperature during deposition and dopant concentration. The study on variation of band gap leads to quantum

confinement effect with heavy doping. The lowest resistivity was 1×10^{-2} Ω cm for the 3 at.% [Al/Zn] film deposited at 475 °C. Hence it can be concluded that, films grown at optimum deposition conditions shows high transmittance and low resistivity. In this study, we have reported the possibility of producing TCO films based on Al-doped ZnO using USP with good electrical and optical properties by optimizing the substrate temperature and doping concentration.

Acknowledgements

The authors wish to thank for the technical assistance of Dr. Jaime Vega Perez, Miguel A. Avendaño, and M.A. Luna-Arias. B.J. Babu is thankful to CONACYT for the scholarship provided to pursue Doctoral program.

References

[1] K.L. Chopra, S. Major, D.K. Pandya, Thin Solid Films 102 (1983) 1–46.
[2] G. Fanga, D. Lia, B.-L. Yaoa, Vacuum 68 (2003) 363–372.
[3] J.H. Lee, B.O. park, Mater. Sci. Eng. B 106 (2004) 242–245.
[4] Mihaela, G.G. Rusu, S.D. Seignon, M. Rusu, Appl. Surf. Sci. 254 (2008) 4179–4185.
[5] S. Fay, U. Kroll, C. Bucher, E. Vallat Sauvain, A. Shah, Sol. Energy Mater. Sol. Cells 86 (2005) 385–397.
[6] H.-M. Zhou, D.-Q. Yi, Z.-M. Yu, L.-R. Xiao, J. Li, Thin Solid Films 515 (2007) 6909–6914.
[7] K.J. Chen, T.H. Fang, F.Y. Hung, L.W. Ji, S.J. Chang, S.J. Young, Y.J. Hsiao, Appl. Surf. Sci. 254 (2008) 5791–5795.
[8] S. Venkatachalam, Y. Iida, Y. Kanno, Superlattices Microstruct. 44 (2008) 127–135.
[9] X. Jiang, F.L. Wong, M.K. Fung, S.T. Lee, Appl. Phys. Lett. 83 (2003) 1875.
[10] K. Liu, B.F. Yang, H. Yan, Z. Fu, M. Wen, Y. Chen, J. Zuo, Appl. Surf. Sci. 255 (2008) 2052–2056.
[11] M.A. Kaid, A. Ashour, Appl. Surf. Sci. 253 (2007) 3029–3033.
[12] T. Prasada Rao, M.C. Santhoshkumar, Appl. Surf. Sci. 255 (2009) 4579–4584.
[13] Y. Lee, H. Kim, Y. Roh, Jpn. J. Appl. Phys. 40 (2001) 2423–2428.
[14] H. Gomez-Pozos, A. Maldonado, M. de la, L. Olvera, Mater. Lett. 61 (2007) 1460–1464.
[15] K. Ernits, D. Brémaud, S. Buecheler, C.J. Hibberd, M. Kaelin, G. Khrypunov, U. Müller, E. Mellikov, A.N. Tiwari, Thin Solid Films 515 (2007) 6051–6054.
[16] S. Buecheler, D. Corica, D. Guettler, A. Chirila, R. Verma, U. Müller, T.P. Niesen, J. Palm, A.N. Tiwari, Thin Solid Films 517 (2009) 2312–2315.
[17] X. Zhang, H. Fan, J. sun, Y. Zhao, Thin Solid Films 515 (2007) 8789–8792.
[18] D.F. Paraguay, L.W. Estrada, D.R. Acosta, M.E. Andrade, M. Yoshida, Thin Solid Films 350 (1999) 192.
[19] M.F. Al-Kuhaili, M.A. Al-Maghrabi, S.M.A. Durrani, I.A. Bakhtiari, J. Phys. D: Appl. Phys. 41 (2008) 215302 (8pp).
[20] P. Prathap, N. Revathi, Y.P. Vsubbaiah, K.T. Ramakrishna Reddy, R.W. Miles, Solid State Sci. 11 (2009) 224–232.
[21] R. Romero, D. Leinen, E.A. Dalchiele, J.R. Ramos-Barrado, F. Martin, Thin Solid Films 515 (2006) 1942–1949.
[22] F. Atay, S. Kose, V. Bilgin, I. Akyuz, Mater. Lett. 57 (2003) 3461–3472.
[23] F. Yakuphanoglu, Y. Caglar, S. Ilican, M. Caglar, Physica B 394 (2007) 86–92.
[24] L. Hadjeris, L. Herissi, M.B. Assouar, T. Easwarakhanthan, J. Bougdira, N. Attaf, M.S. Aida, Semiconduct. Sci. Technol. 24 (2009) 035006 (6pp).
[25] A.F. Aktaruzzaman, G.L. Sharma, L.K. Malhotra, Thin Solid Films 198 (1991) 67–74.
[26] B. Joseph, P.K. Manoj, V.K. Vaidyan, Ceram. Int. 32 (2006) 487–493.
[27] B. Ergin, E. Ketenci, F. Atay, Int. J. Hydrogen Energy (2008) 1–6.
[28] V. Srikant, D.R. Clarke, J. Mater. Res. 12 (6) (1997) 1425–1428.
[29] H. Gomez, A. Maldonado, R. Casatanedo-perez, G. Torres-Delgado, M. de La, L. Olvera, Mater. Charact. 58 (2007) 708–714.
[30] S. Yanfeng, W. Liu, H. Zhidan, L. Shaolin, Z.Z. Yi, G. Du, Vacuum 80 (2006) 981–985.